Bioorganic Chemistry 87 (2019) 629–637

Contents lists available at ScienceDirect

Bioorganic Chemistry

journal homepage: www.elsevier.com/locate/bioorg

Tick-borne flavivirus reproduction inhibitors based on isoxazole core linked with adamantane

Dmitry A. Vasilenko[a], Evgenia V. Dueva[a,b,1], Liubov I. Kozlovskaya[b,c], Nikolay A. Zefirov[a,d], Yuri K. Grishin[a], Gennady M. Butov[e], Vladimir A. Palyulin[a,d], Tamara S. Kuznetsova[a], Galina G. Karganova[b,c], Olga N. Zefirova[a,d], Dmitry I. Osolodkin[a,b,c,*], Elena B. Averina[a,d,*]

[a] Department of Chemistry, Lomonosov Moscow State University, Leninskie Gory 1 bd. 3, Moscow 119991, Russia
[b] FSBSI "Chumakov FSC R&D IBP RAS", Moscow 108819, Russia
[c] Sechenov First Moscow State Medical University, Moscow 119991, Russia
[d] Institute of Physiologically Active Compounds, Severny Proezd 1, Chernogolovka, Moscow Region 142432, Russia
[e] Volgograd State Technical University, Lenina Avenue 28, Volgograd 400005, Russia

ARTICLE INFO

Keywords:
Aminoisoxazoles
Adamantane derivatives
Tick-borne encephalitis virus
Omsk hemorrhagic fever virus
Powassan virus
Flavivirus

ABSTRACT

Infections caused by flaviviruses pose a huge threat for public health all over the world. The search for therapeutically relevant compounds targeting tick-borne flaviviruses requires the exploration of novel chemotypes. In the present work a large series of novel polyfunctionalized isoxazole derivatives bearing substituents with various steric and electronic effects was obtained by our unique versatile synthetic procedure and their antiviral activity against tick-borne encephalitis, Omsk hemorrhagic fever, and Powassan viruses was studied *in vitro*. The majority of studied isoxazoles showed activity in low micromolar range. No appreciable cytotoxicity was observed for tested compounds. The lead compounds, 5-aminoisoxazole derivatives containing adamantyl moiety, exhibited strong antiviral activity and excellent therapeutic index.

1. Introduction

Flaviviral (genus *Flavivirus,* family *Flaviviridae*) infections, such as dengue fever, West Nile disease, Zika fever, yellow fever, Japanese encephalitis, tick-borne encephalitis, etc., pose a huge threat for public health all over the world. Vaccines are available only against yellow fever, Japanese encephalitis, and tick-borne encephalitis, but they can be used only as preventive measures. The situation is complicated by the absence of any anti-flaviviral drugs, and only symptomatic treatment of flaviviral diseases is practiced. Though mosquito-borne flaviviral diseases are more incident and spread all over the world, tick-borne flaviviruses are especially important for public health in the Northern hemisphere. Tick-borne encephalitis virus (TBEV) causes up to 10,000 cases every year in the Northern Eurasia. Powassan virus (POWV) and Omsk hemorrhagic fever virus (OHFV) are of local importance. With the global climate changes in the last decades, ticks moved further north, and the incidence and area of tick-borne flaviviral diseases increased dramatically [1–3], raising an urgent need for new antiflavivirals.

A widely used strategy of design of antivirals against enveloped viruses, including flaviviruses, is the inhibition of virus entry into the host cells through prevention of the fusion between cellular and virion membranes (reviewed in [3]). One of the possible molecular targets for flavivirus fusion inhibitors is the envelope protein E, involved in this process. Earlier we constructed a homology model for tick-borne encephalitis virus E protein based on template structures with a detergent *n*-octyl-β-D-glucoside (β-OG) molecule bound in a hydrophobic pocket [4]. Small molecules may occupy the pocket and prevent conformational rearrangement of the E protein, required for the membrane fusion and viral genome release into cytoplasm.

As far as the protein composition and structure of flaviviruses, especially tick-borne ones, are rather conserved [5], TBEV fusion inhibitors can be expected to inhibit the reproduction of other group members as broad-spectrum antivirals.

Abbreviations: β-OG, *n*-octyl-β-D-glucoside; TBEV, tick-borne encephalitis virus; OHFV, Omsk hemorrhagic fever virus; POWV, Powassan virus; PEK, porcine embryo kidney; FBS, fetal bovine serum

* Corresponding authors: FSBSI "Chumakov FSC R&D IBP RAS", Poselok Instituta Poliomielita 8 bd. 1, Poselenie Moskovsky, 108819 Moscow, Russian Federation. Tel.: +7-495-841-02-02.

E-mail addresses: dmitry_o@qsar.chem.msu.ru (D.I. Osolodkin), elaver@med.chem.msu.ru (E.B. Averina).

[1] Present address: Vancouver Prostate Centre, Department of Urologic Sciences, The University of British Columbia, Vancouver, V6H 3Z6 BC, Canada.

https://doi.org/10.1016/j.bioorg.2019.03.028
Received 11 December 2018; Received in revised form 22 February 2019; Accepted 13 March 2019
Available online 16 March 2019
0045-2068/ © 2019 Elsevier Inc. All rights reserved.

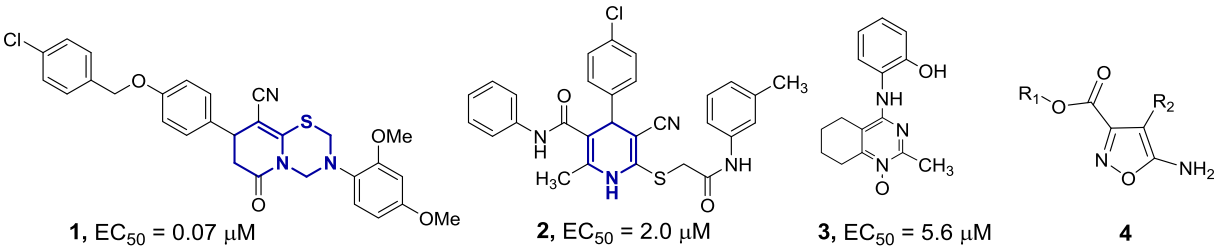

Fig. 1. Examples of TBEV fusion inhibitors studied earlier (**1–3**) and in the present work (**4**).

Representatives of several chemical classes were assessed against flavivirus reproduction at the stage of entry. Various heterocyclic compounds, rigid amphipathic fusion inhibitors (RAFIs), organoselenium compounds showed activity in micromolar range and lower (reviewed in [1]).

Previously, our search for structurally different inhibitors of TBEV reproduction based on the results of virtual or exploratory screening [4,6–12] revealed the pronounced antiviral activity of derivatives of pyrido[2,1-*b*][1,3,5]thiadiazines (e.g., **1**, Fig. 1), while a search among 1,4-dihydropyridines (e.g., **2**) or 4-aminotetrahydroquinazoline *N*-oxides (e.g., **3**) led to less potent and rather toxic compounds.

As the enhancement of structural diversity provides opportunities for the development of antiflavivirals with greater therapeutic potential, in the present work we aimed to synthesize a novel series of compounds based on a scaffold never assessed against flaviviruses and to study their activity against tick-borne flaviviruses (TBEV, POWV, OHFV). We studied the isoxazole-based compounds of general formula **4** (Fig. 1) due to their structural compactness, synthetic availability, and possibility of diverse functionalization.

2. Results and discussion

2.1. Chemistry

The synthesis of a series of novel 5-aminoisoxazoles **4a-o** with various structures was performed using a three-step synthetic procedure based on our previously described method [13–17]. The route to target compounds **4a-o** includes the preparation of unsaturated esters **5a-o**, their subsequent heterocyclization under the treatment with activated tetranitromethane, followed by the reduction of 5-nitroisoxazoles **6a-o** (Table 1). The majority of starting alkenes (**5c-n**) was synthesized by the acylation of corresponding alcohol in the presence of a base. The ester **5o** was obtained by Wittig reaction from the phosphonium ylide of 1-adamantylmethyl iodoacetate and 3-phenylpropanal. All synthesized compounds were characterized and identified using ^{1}H and ^{13}C NMR spectroscopy, and HRMS or elemental analysis.

2.2. Cytotoxicity and antiviral activity

Based on the data obtained in our previous studies and aiming to find flavivirus fusion inhibitors that may interact with the β-OG pocket of the E protein, we challenged isoxazole derivatives **4a-o** with different lipophilic moieties at positions 3 and 4 of heterocycle against TBEV, POWV, and OHFV reproduction in *in vitro* plaque formation inhibition test, and 50% effective concentrations were calculated (EC_{50}). The viruses were studied in the same permissive porcine embryo kidney (PEK) cell line and conditions. Cytotoxicity was estimated in the same cell line for active compounds as the concentration causing death of 50% of the cell monolayer (CC_{50}) acutely (24 h exposition) and chronically (7 days exposition).

Compounds **4a-d**, bearing lipophilic *tert*-butyl, benzyl, 1-adamantyl or 2-adamantyl moieties in the ester groups, showed similar moderate anti-flavivirus activity (Table 2). The EC_{50} values were the lowest for both 1-adamantyl and 2-adamantyl containing isoxazole derivatives **4c,d** and did not depend on the position of the adamantyl substitution. However, the 1-adamantyl derivative **4c** was less toxic than **4d**.

To probe the additional modifications of the 1-adamantyl moiety, we introduced there the substituents with different steric and electronic effects (compounds **4e-h, 6h**) or replaced it with a more flexible bicyclo [3.3.1]nonane moiety (compound **4i**, analogous to adamantyl containing heterocycle **4e**, Table 3). The introduction of the substituents into adamantane core, regardless of their type, bulkiness, number, and positions, did not lead to improvement of antiviral properties as compared to the parent compound **4c**. Both carbomethoxy derivatives **4i** and **4e** with different conformational flexibility of the polycyclic moiety were inactive against studied tick-borne flaviviruses. Addition of an acetamide to the adamantyl also rendered the compounds inactive (**4h**, **6h**).

More successful against TBEV reproduction was the modification of the linker between the isoxazole and adamantane fragments (Table 4). The elongation of the linker by one methylene group (**4j**) led to a substantial increase in the antiviral activity, about one order of magnitude. Further elongation and/or modification of the linker, including its conformational restriction, did not improve the activity against TBEV (**4k-m**). The activity of the studied subseries against OHFV and POWV reproduction was less prominent.

The synthetic precursor of heterocycle **4j**, corresponding 5-nitroisoxazole **6j**, showed a significant antiviral activity decrease, confirming the importance of the presence of the amino group in the heterocycle. Finally, the introduction of a lipophilic β-phenylethyl substituent in the position 4 of the isoxazole ring (**4o**) not only maintained reasonable antiviral properties against TBEV, but markedly reduced the toxicity compared to **4j**. Moreover, the activity of **4o** against OHFV reproduction was the highest from the whole series. Thus, the therapeutic index of **4o** was the best in the studied series of isoxazole derivatives (Table 5).

2.3. Mechanism of action studies

A 'time-of-addition' experiment was performed to elucidate the stage of flavivirus replication cycle inhibited by the compounds. During this experiment the compounds were added to the infected cells at different stages of viral replication cycle to elucidate the inhibited stage that decreases viral reproduction the most. The experiment was performed using TBEV only. We compared the effect of compound addition on the several stages of viral replication cycle: before infection on cells or virions (viral adsorption and entry, including fusion), on viral protein synthesis, and viral genome replication. To achieve that, we estimated and compared with the control the viral yields after infection of the cells with TBEV after pretreatment of the cells with solutions of the compounds with concentration of 5 × EC_{50}, virus preincubation with the compounds, or when a compound solution was added at the start of viral protein synthesis at 2 h post infection (h.p.i.) or at the start of viral genome replication at 5 h.p.i. Two potent compounds with different EC_{50} values, **4b** (EC_{50} 19 μM) and **4o** (EC_{50} 3.7 μM), were studied, DMSO-treated cells were used as a control, and the results were summarized in Fig. 2.

Addition of a compound solution 2 or 5 h.p.i. did not inhibit viral

Table 1
Three-step procedure for the synthesis of 5-aminoisoxazoles **4a-o**.

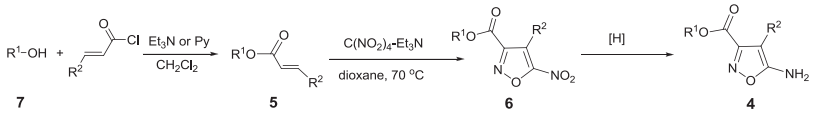

R^1	R^2	Compounds 7	Compounds 4–6	Yield, %[a]		
				5	6	4
t-Bu	H	**a**	**a**	–[b]	75[c]	45 (A)[c]
$PhCH_2$	H	**b**	**b**	–[b]	36[c]	72 (A)[c]
	H	**c**	**c**	84[c]	57[c]	62 (A)
	H	**d**	**d**	90[c]	58[c]	67 (A)
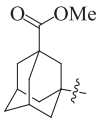	H	**e**	**e**	52	44	55 (A)
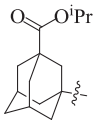	H	**f**	**f**	61[c]	33[c]	68 (A)
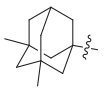	H	**g**	**g**	54[c]	63[c]	34 (A)
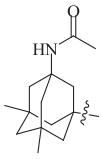	H	**h**	**h**	43	32	65 (B)
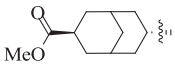	H	**i**	**i**	50	44	49 (B)
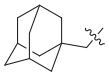	H	**j**	**j**	83[c]	68[c]	75[c] (A)
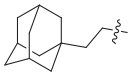	H	**k**	**k**	78[c]	84[c]	78 (A)
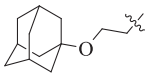	H	**l**	**l**	72[c]	55[c]	52 (A)
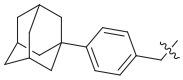	H	**m**	**m**	82[c]	36[c]	56 (A)
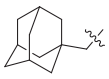	Me	**j**	**n**	78	54	74 (B)
	CH_2CH_2Ph	**j**	**o**	84[d]	37	64 (B)

[a] Isolated yields after chromatographic purification.
[b] Commercially available.
[c] Compounds were synthesized by known procedures [15,16].
[d] Alkene **5o** was synthesized by Wittig reaction (see Supplementary material).

reproduction. Virus exposition to the compound before the interaction with the cells significantly decreased virus growth in comparison with DMSO-treated control. The effect was the most pronounced upon the preincubation of the virus with a compound, implying the direct interaction of the compound with the virion. However, the preincubation of the cells with the compound decreased viral yields as well. Thus, we can expect a compound to interact with the cellular targets involved into viral attachment and entry. Nevertheless, compounds inhibit viral replication cycle on the first stages, similarly to the results of the previous studies. Most likely, the compounds do interact with the E protein molecule, as it is the only one fully exposed on the flavivirus virion surface.

Table 2
Cytotoxicity and antiviral activity of the compounds with variations of the lipophilic moiety.

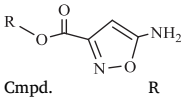

Cmpd.	R	CC_{50}, μM		anti-TBEV EC_{50}, μM	anti-OHFV EC_{50}, μM	anti-POWV EC_{50}, μM
		24 h	7 days			
4a	*t*-Bu	> 500	> 500	17 ± 3	> 50	13 ± 3
4b	$PhCH_2$	> 500	324	19 ± 6	> 50	31 ± 7
4c		> 500	382	11 ± 4	26 ± 1	12 ± 5
4d		350	160	11 ± 2	30 ± 1	13 ± 6
Ref. [12]	*N*-Butyl-2-methyl-5,6,7,8-tetrahydroquinazoline-4-amine 1-oxide	> 50	> 50	12 ± 1	ND	ND

ND, not determined.

Table 3
Cytotoxicity and antiviral activity of the compounds with variations in the adamantane core.

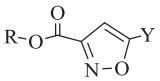

Cmpd.	R	Y	CC_{50}, μM		anti-TBEV EC_{50}, μM	anti-OHFV EC_{50}, μM	anti-POWV EC_{50}, μM
			24 h	7 days			
4e		NH_2	ND	ND	> 50	> 50	> 50
4f		NH_2	> 500	> 500	29 ± 3	> 50	18 ± 7
4g		NH_2	354	354	13 ± 2	22 ± 5	8 ± 2
6h	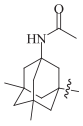	NO_2	ND	ND	> 50	ND	ND
4h	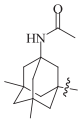	NH_2	ND	ND	> 50	> 50	> 50
4i	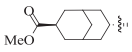	NH_2	ND	ND	> 50	> 50	> 50

ND, not determined.

Table 4
Cytotoxicity and antiviral activity of the compounds with linker variations.

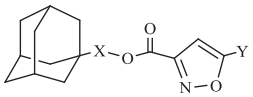

Cmpd.	X	Y	CC_{50}, μM		anti-TBEVEC_{50}, μM	anti-OHFVEC_{50}, μM	anti-POWVEC_{50}, μM
			24 h	7 days			
4j	$-CH_2-$	NH_2	88	88	1.7 ± 0.1	24 ± 3	24 ± 8
6j	$-CH_2-$	NO_2	ND[a]	ND[a]	17 ± 3	ND	ND
4k	$-CH_2-CH_2-$	NH_2	> 500	416	14 ± 2	13 ± 5	12 ± 2
4l	$-O-CH_2-CH_2-$	NH_2	ND	ND	> 50	> 50	38 ± 12
4m	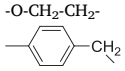	NH_2	386	273	20 ± 3	22 ± 20	29 ± 5

[a] CC_{50} was not determined due to the ability of **6j** to cause the cytoskeleton disruption. ND, not determined

Table 5
Cytotoxicity and antiviral activity of the compounds with variation of the isoxazole core.

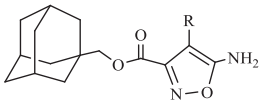

Cmpd.	R	CC_{50}, μM		anto-TBEVEC_{50}, μM	anti-OHFV,EC_{50}, μM	anti-POWVEC_{50}, μM
		24 h	7 days			
4n	Me	118	62	22.4 ± 0.6	25 ± 5	14 ± 3
4o	CH_2CH_2Ph	> 500	416	3.7 ± 0.2	12 ± 2	15 ± 2

2.4. Docking studies

Docking studies were performed to investigate possible binding modes of all the studied compounds in β-OG pocket of TBEV E protein. The homology model, structure preparation and docking protocol were the same as in the previous study [12]. The β-OG pocket has the shape of a funnel open to the space surrounding the virus particle (Fig. 3). Majority of the compounds, bearing isoxazole warhead unsubstituted in the position 4, were docked in an orientation with the warhead buried deep in the pocket and forming hydrogen bonds with Gln214 amide group and Val273 backbone carbonyl (Fig. 3A and B). Adamantyl substituent is largely exposed to the environment and may form hydrophobic interactions; however, the entrance to the pocket is open enough to allow different substitutions without substantial changes in the binding mode. That explains the limited influence of the adamantyl modification on the activity.

On the other hand, compound **4o** bears a bulky substituent in the position 4 of the isoxazole ring. Thus, realization of the common binding mode becomes impossible due to a very limited volume of the funnel, and the compound binds mostly on the periphery of the pocket (Fig. 3C and D). In this binding mode, a hydrogen bond is predicted between the isoxazole oxygen and Tyr132 phenolic hydroxyl. Such a binding mode appears to be more susceptible to the amino acid variability, which is more common for the pocket periphery than for its deep region. Additional substituent extending into the pocket could improve the binding between the compound and the E protein.

The results of the docking modeling are consistent with the possibility of binding the suggested compounds in the β-OG pocket.

2.5. Predicted ADMET profiles and physico-chemical properties of compounds

In order to assess the suitability of the synthesized compounds for the *in vivo* studies, we have performed a preliminary computational estimation of certain ADMET and physico-chemical properties, relevant in the drug development context. In particular, the human intestinal absorption (HIA) [18], blood-brain barrier permeability (LogBB) [19], and hERG-mediated cardiac toxicity risk (channel affinity pK_i and inhibitory activity pIC_{50}) [20] were estimated using the predictive QSAR models based on the accurate and representative training sets, fragmental descriptors, and artificial neural networks. The lipophilicity ($logP_{ow}$) for the neutral compound and the aqueous solubility (pS) were estimated by the ALogPS 3.0 neural network model based on the E-State descriptors implemented in the OCHEM platform [21]. The predicted properties of the compounds (Supplementary Table S1) seem to be reasonable for early lead candidates, including excellent intestinal absorption, medium or low blood-brain barrier permeability, acceptable hERG liability risks, as well as moderate lipophilicity and good solubility. Moreover, the ADMET properties will be inevitably optimized at later stages of the development.

3. Conclusion

A series of novel isoxazole derivatives was synthesized and tested for activity against TBEV, OHFV, and POWV reproduction *in vitro*. These heterocycles represent a novel type of small-molecule inhibitors of flaviviruses. The investigation led to the discovery of two potent and synthetically accessible 5-aminoisoxazole derivatives containing adamantyl moiety, one of them possessing an attractive therapeutic index. Realization of the antiviral activity on the virus attachment and entry

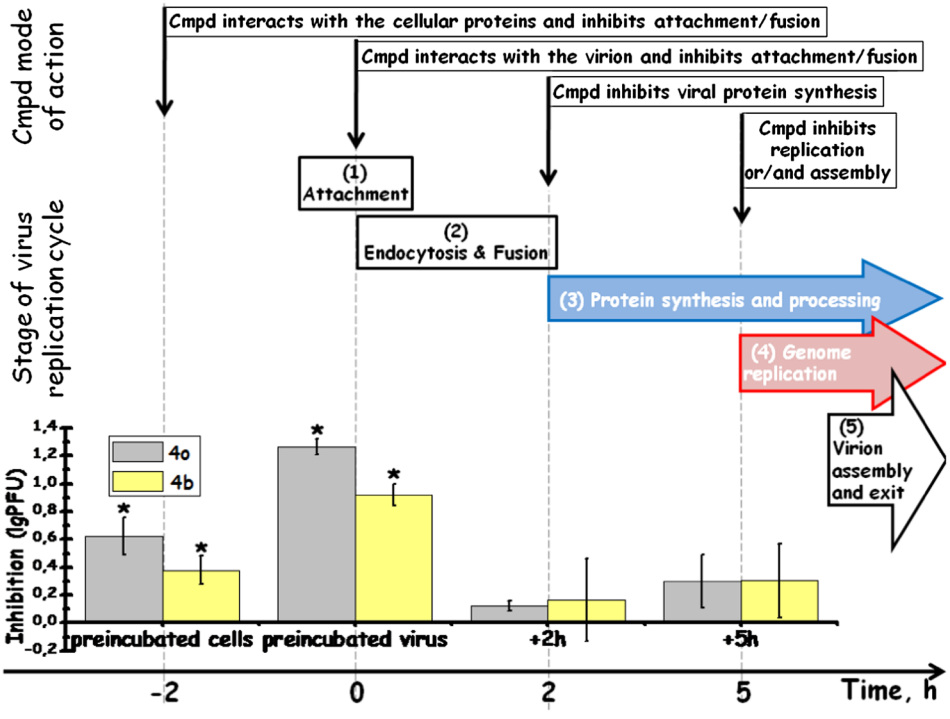

Fig. 2. 'Time of addition': Comparison of the viral yields on the control DMSO-treated cells after infection with TBEV (MOI 0.1 PFU/cell) with viral yields on the cells treated with compounds **4b** or **4o** (5 × EC_{50}, 95 and 18.5 μM) on the various stages of infection. (* – inhibition is statistically significant in comparison with a DMSO-treated control).

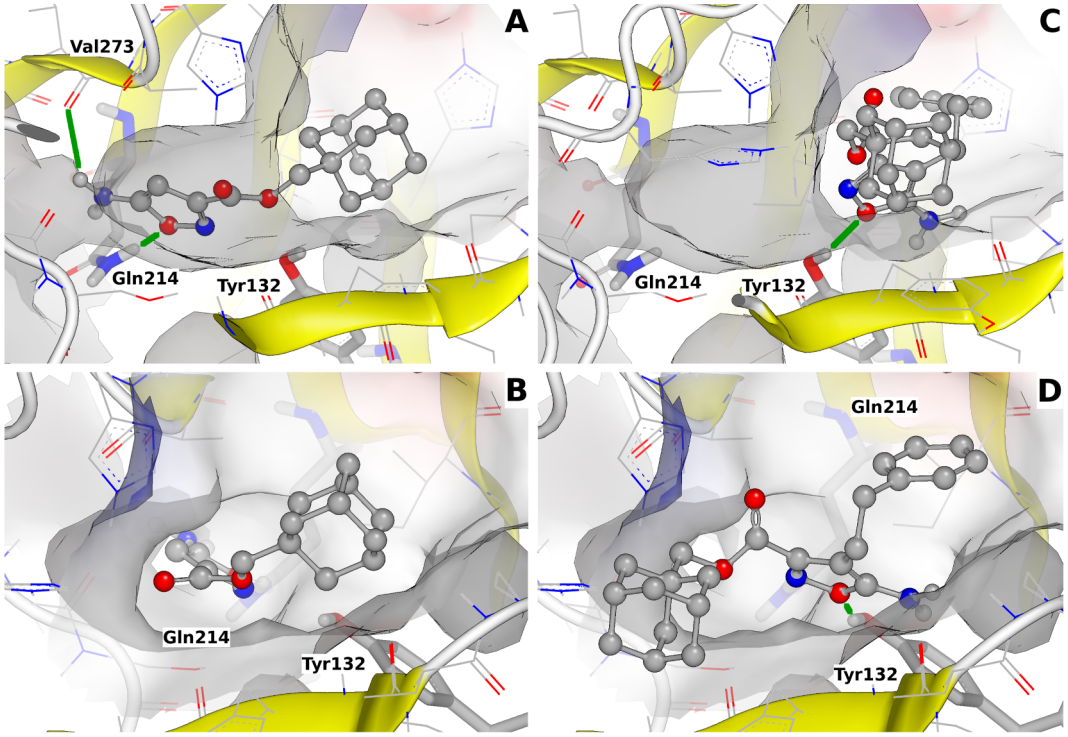

Fig. 3. Predicted binding modes of compounds **4j** (A, B) and **4o** (C, D) in β-OG pocket of TBEV E protein. Panels A, C: side view (environment on the right, virus membrane on the left). Panels B, D: view from outside. Hydrogen bonds predicted by VIDA 'FRED view' are shown as green lines and participating amino acid residues are inscribed.

stages was confirmed by the 'time-of-addition' experiments. Studied heterocycles may be considered as a promising and useful scaffold for the further optimization of antiviral activity.

4. Experimental section

4.1. Chemistry

4.1.1. General information

NMR spectra were recorded on the Agilent 400-MR spectrometer (400.0 MHz for ^{1}H; 100.6 MHz for ^{13}C, 161.9 MHz for ^{31}P) at room temperature; chemical shifts (δ) were measured with reference to the solvent $CDCl_3$ for ^{1}H (δ = 7.26 ppm) and ^{13}C (δ = 77.1 ppm), and 85% H_3PO_4 for ^{31}P as external standard. Chemical shifts (δ) are given in ppm; *J* values are given in Hz. When necessary, assignments of signals in NMR spectra were made using 2D techniques. Accurate mass measurements (HRMS) were performed on a Bruker micrOTOF II instrument using electrospray ionization (ESI). The measurements were done in a positive ion mode (interface capillary voltage 4500 V) or in a negative ion mode (3200 V). Analytical thin layer chromatography was carried out with Silufol silica gel plates (supported on aluminum); the detection was done by UV lamp (254 and 365 nm) and chemical staining (5% aqueous solution of $KMnO_4$). Column chromatography was performed on silica gel (230–400 mesh, Merck). Compounds **4a** [16], **4b** [16], **4j** [15], **5c** [16], **5d** [16], **5f** [16], **5g** [16], **5j** [16], **5k** [16], **5l** [16], **5m** [16], **6a** [16], **6b** [16], **6c** [16], **6d** [16], **6f** [16], **6g** [16], **6j** [22], **6k** [16], **6m** [16], **7c** [23], **7d** [24], **7e** [25,26], **7f** [25,26], **7g** [27], **7h** [28–30], **7i** [31], **7j** [32], **7k** [33], **7l** [34], and **7m** [35] were synthesized by known procedures.

All other starting materials were commercially available.

All reagents except commercial products of satisfactory quality were purified by literature procedures prior to use.

4.1.2. General procedure for the preparation of compounds *4a-o*

Method A: To a stirred solution of 5-nitroisoxazole (0.3 mmol) in 96% EtOH (1 mL), $SnCl_2$ (285 mg, 1.5 mmol) was added in one portion. The reaction mixture was stirred for 2 h at r.t., then the solvent was evaporated *in vacuo* and the residue was dissolved in CH_2Cl_2 (20 mL) and washed with sat. aq $NaHCO_3$ (resulting in a solution at pH 8). The aqueous phase was extracted with CH_2Cl_2 (3 × 10 mL) and the combined organic layers were dried over $MgSO_4$. The solvent was evaporated *in vacuo* and the residue was purified by preparative column chromatography on silica gel.

Method B: To a stirred solution of 5-nitroisoxazole (0.3 mmol) in a mixture (1:1) THF-H_2O (2 mL) $Na_2S_2O_4$ (392 mg, 1.8 mmol) was added in one portion at room temperature. The resulting mixture was stirred for 1 h at 90 °C. Then the mixture was cooled to room temperature, water (5 mL) was added and extracted with EtOAc (3 × 10 mL). The combined organic layers were dried over anhydrous $MgSO_4$. The solvent was evaporated in vacuo; the residue was purified by preparative column chromatography on silica gel.

*4.1.2.1. 1-Adamantyl 5-aminoisoxazole-3-carboxylate (**4c**).* Colourless solid (49 mg, 62%, A), mp: 188–190 °C, R_f (petroleum ether/EtOAc 2:1): 0.20; ^{1}H NMR (400.0 MHz, $CDCl_3$) (δ, ppm): 1.62–1.72 (m, 6H, $2CH_2$(Ad)), 2.16–2.20 (m, 3H, 3CH(Ad)), 2.20–2.24 (m, 6H, $3CH_2$(Ad)), 4.63 (br.s, 2H, NH_2), 5.44 (s, 1H, CH); ^{13}C NMR (100.6 MHz, $CDCl_3$) (δ, ppm): 30.9 (3CH(Ad)), 36.1 ($3CH_2$(Ad)), 41.2 ($3CH_2$(Ad)), 80.7 (CH), 83.2 (C(Ad)), 158.8 (C), 159.1 (C═O), 169.4 (CNH_2); HRMS-ESI *m/z* $[M+H]^+$ calcd for $C_{14}H_{19}N_2O_3^+$: 263.1390, found 263.1390; Anal. calcd for $C_{14}H_{18}N_2O_3$: C 63.11, H 6.92, N 10.68, found: C 63.98, H 7.15, N 10.63.

*4.1.2.2. 2-Adamantyl 5-aminoisoxazole-3-carboxylate (**4d**).* Colourless solid (53 mg, 67%, A), mp: 171–174 °C, R_f (petroleum ether/EtOAc 3:1): 0.30; ^{1}H NMR (400.0 MHz, $CDCl_3$) (δ, ppm): 1.52–1.60 (m, 2H, $2CH_2$(Ad)), 1.69–1.74 (m, 2H, $2CH_2$(Ad)), 1.74–1.81 (m, 2H,

$2CH_2$(Ad)), 1.81–1.90 (m, 4H, 2CH + CH_2(Ad)), 2.03–2.14 (m, 4H, $2CH_2$ (Ad) + 2CH(Ad)), 4.86 (br.s, 2H, NH_2), 5.11–5.15 (m, 1H, CHO), 5.50 (s, 1H, CH); ^{13}C NMR (100.6 MHz, $CDCl_3$) (δ, ppm): 26.9 (CH (Ad)), 27.1 (CH(Ad)), 31.7 ($2CH_2$(Ad)), 31.8 (2CH(Ad)), 36.2 ($2CH_2$(Ad)), 37.2 (CH_2(Ad)), 78.9 (CHO), 80.7 (CH), 157.9 (C), 159.8 (C═O), 169.9 (CNH_2); HRMS-ESI *m/z* $[M+Na]^+$ calcd for $C_{14}H_{18}N_2O_3Na^+$: 283.1210, found: 285.1210. Anal. calcd for $C_{14}H_{18}N_2O_3$: C 63.11, H 6.92, N 10.68, found: C 63.42, H 7.23, N 10.36.

4.1.2.3. 3-(Methoxycarbonyl)-1-adamantyl 5-aminoisoxazole-3-carboxylate ***(4e)***. Colourless solid (53 mg, 55%, A), mp: 166–167 °C, R_f (petroleum ether/EtOAc 2:1): 0.20; ^{1}H NMR (400.0 MHz, $CDCl_3$) (δ, ppm): 1.57–1.68 (m, 2H, CH_2(Ad)), 1.81–1.88 (m, 4H, $2CH_2$(Ad)), 2.14–2.20 (m, 2H, $2CH_2$(Ad)), 2.20–2.26 (m, 2H, $2CH_2$(Ad)), 2.27–2.32 (m, 2H, 2CH(Ad)), 2.34 (br.s, 2H, CH_2(Ad)), 3.64 (s, 3H, CH_3), 4.70 (br.s, 2H, NH_2), 5.43 (s, 1H, CH); ^{13}C NMR (100.6 MHz, $CDCl_3$) (δ, ppm): 30.3 (2CH(Ad)), 35.0 (CH_2(Ad)), 37.7 ($2CH_2$(Ad)), 40.2 ($2CH_2$(Ad)), 42.2 (CH_2(Ad)), 44.1 (C(Ad)), 51.8 (C—O), 80.5 (CH), 82.5 (CH_3), 158.5 (C), 159.0 (C═O), 169.6 (CNH_2)0.176.4 (C═O); HRMS-ESI *m/z* $[M+H]^+$ calcd for $C_{16}H_{21}N_2O_6^+$: 321.1445, found: 321.1444; Anal. calcd for $C_{16}H_{20}N_2O_5$: C 59.99, H 6.29, N 8.74, found: C 59.85, H 6.38, N 8.42.

4.1.2.4. 3-(i-Propoxycarbonyl)-1-adamantyl 5-aminoisoxazole-3-carboxylate ***(4f)***. Colourless solid (71 mg, 68%, A), mp: 177–178 °C, R_f (petroleum ether/EtOAc 2:1): 0.42; ^{1}H NMR (400.0 MHz, $CDCl_3$) (δ, ppm): 1.18 (d, J = 6.3 Hz, 6H, $2CH_3$), 1.58–1.70 (m, 2H, CH_2(Ad)), 1.77–1.87 (m, 4H, $2CH_2$(Ad)), 2.13–2.20 (m, 2H, $2CH_2$(Ad)), 2.23–2.28 (m, 2H, $2CH_2$(Ad)), 2.28–2.33 (m, 4H, CH_2(Ad) + 2CH(Ad)), 4.64 (br.s, 2H, NH_2), 4.95 (sept, J = 6.3 Hz, 1H, OCH), 5.45 (s, 1H, CH); ^{13}C NMR (100.6 MHz, $CDCl_3$) (δ, ppm): 21.7 ($2CH_3$), 30.4 (2CH(Ad)), 35.0 (CH_2(Ad)), 37.6 ($2CH_2$(Ad)), 40.2 ($2CH_2$(Ad)), 42.2 (CH_2(Ad)), 44.0 (C(Ad)), 67.5 (CH—O), 80.6 (CH), 82.7 (C—O), 158.5 (C), 159.0 (C═O), 169.5 (CNH_2)0.175.4 (C═O); HRMS-ESI *m/z* $[M+H]^+$ calcd for $C_{18}H_{25}N_2O_5^+$: 349.1758; found 349.1755; Anal. calcd for $C_{18}H_{24}N_2O_5$: C 62.05, H 6.94, N 8.04, found: C 61.93, H 6.71, N 7.78.

4.1.2.5. 3,5-Dimethyl-1-adamantyl 5-aminoisoxazole-3-carboxylate ***(4g)***. Colourless solid (30 mg, 34%, A), mp: 146–148 °C, R_f (petroleum ether/EtOAc 4:1): 0.24; ^{1}H NMR (400.0 MHz, $CDCl_3$) (δ, ppm): 0.86 (s, 6H, $2CH_3$), 1.09–1.23 (m, 2H, CH_2 (Ad)), 1.24–1.31 (m, 2H, $2CH_2$(Ad)), 1.35–1.41 (m, 2H, $2CH_2$(Ad)), 1.79–1.91 (m, 4H, $2CH_2$(Ad)), 2.05 (br.s, 2H, CH_2(Ad)), 2.20–2.25 (m, 1H, CH(Ad)), 4.77 (s, 2H, NH_2), 5.41 (s, 1H, CH); ^{13}C NMR (100.6 MHz, $CDCl_3$) (δ, ppm): 29.8 ($2CH_3$), 31.2 (CH (Ad)), 34.1 (2C(Ad)), 39.6 (CH_2(Ad)), 42.4 ($2CH_2$(Ad)), 47.1 ($2CH_2$(Ad)), 50.4 (CH_2(Ad)), 80.5 (CH), 84.5 (C (Ad)), 158.7 (C), 159.2 (C═O), 169.6 (C—NH_2). Anal. calcd for $C_{16}H_{22}N_2O_3$: C 66.18, H 7.64, N 9.65, found: C 66.17, H 7.31, N 9.53.

4.1.2.6. 3-(Acetylamino)-5,7-dimethyl-1-adamantyl 5-aminoisoxazole-3-carboxylate ***(4h)***. Colourless solid (68 mg, 65%, B), mp: 119–122 °C, R_f ($CHCl_3$/MeOH 20:1): 0.35; ^{1}H NMR (400.0 MHz, $CDCl_3$) (δ, ppm): 0.93 (s, 6H, $2CH_3$), 1.12–1.20 (m, 2H, CH_2(Ad)), 1.59–1.65 (m, 2H, $2CH_2$(Ad)), 1.67–1.73 (m, 2H, $2CH_2$(Ad)), 1.81–1.92 (m, 4H, $2CH_2$(Ad), 1.86 (s, 3H, CH_3), 2.35 (br.s, 2H, CH_2(Ad)), 4.79 (br.s, 2H, NH_2), 5.34 (br.s 1H, NH), 5.40 (s, 1H, CH); ^{13}C NMR (100.6 MHz, $CDCl_3$) (δ, ppm): 24.5 (CH_3), 29.0 ($2CH_3$), 34.2 (2C(Ad)), 43.5 (CH_2(Ad)), 46.1 ($2CH_2$(Ad)), 46.4 ($2CH_2$(Ad)), 49.3 (CH_2(Ad)), 54.9 (C(Ad)), 80.4 (CH), 83.6 (C(Ad)), 158.4 (C), 159.1 (C═O), 169.6 (C), 169.7 (C); HRMS-ESI *m/z* $[M+H]^+$ calcd for $C_{18}H_{26}N_3O_4^+$: 348.1918, found: 348.1918.

4.1.2.7. (3r,7r)-7-(Methoxycarbonyl)bicyclo[3.3.1]non-3-yl 5-aminoisoxazole -3-carboxylate ***(4i)***. Colourless solid (45 mg, 49%, B), mp: 177–178 °C, R_f (petroleum ether/EtOAc 4:1): 0.10; ^{1}H NMR (400.0 MHz, $CDCl_3$) (δ, ppm): 1.32–1.40 (m, 1H, CH_2), 1.57–1.72 (m, 5H, $5CH_2$), 1.82–1.91 (m, 2H, $2CH_2$), 2.19–2.26 (m, 2H, 2CH), 2.25 (ddd, J = 14.6, 8.6, 6.9 Hz, 2H, $2CH_2$), 3.25 (J = 12.8, 5.1 Hz , 1H, CH—C═O), 3.70 (s, 3H, CH_3), 4.64 (br. s, 2H, NH_2), 5.29 (quint, J = 6.8 Гц, 1H, OCH), 5.57 (s, 1H, CH); ^{13}C NMR (100.6 MHz, $CDCl_3$) (δ, ppm): 25.8 (2CH), 29.8 (CH_2), 32.8 ($2CH_2$), 34.1 (2CH), 34.4 (CH_2), 51.5 (CH—O), 69.3 (CH_3), 80.5 (CH), 157.7 (C), 159.8(C═O), 169.6 (C—NH_2), 177.7 (C═O); HRMS-ESI *m/z* $[M+K]^+$ calcd for $C_{15}H_{20}N_2O_5K^+$: 347.1004, found: 347.1003.

4.1.2.8. 2-(1-Adamantyl)ethyl 5-aminoisoxazole-3-carboxylate ***(4k)***. Colourless solid (68 mg, 78%, A), mp: 152–154 °C, R_f (petroleum ether/EtOAc 3:1): 0.34; ^{1}H NMR (400.0 MHz, $CDCl_3$) (δ, ppm): 1.50–1.56 (m, 8H, $3CH_2$(Ad) + CH_2), 1.57–1.64 (m, 3H, $3CH_2$(Ad)), 1.64–1.72 (m, 3H, $3CH_2$(Ad)), 1.90–1.96 (m, 3H, 3CH(Ad)), 4.36 (t, J = 7.4 Hz, 2H, OCH_2), 4.69 (br.s, 2H, NH_2), 5.50 (s, 1H, CH); ^{13}C NMR (100.6 MHz, $CDCl_3$) (δ, ppm): 28.5 (3CH(Ad)), 31.8 (C(Ad)), 36.9 ($3CH_2$(Ad)), 42.1 (CH_2), 42.4 ($3CH_2$(Ad)), 62.4 (CH_2O), 80.6 (CH), 157.5 (C), 160.5 (C═O), 169.6 (CNH_2); HRMS-ESI *m/z* $[M+Na]^+$ calcd for $C_{16}H_{22}N_2O_3Na^+$: 313.1523, found: 313.1532; Anal. calcd for $C_{16}H_{22}N_2O_3$: C 66.18, H 7.64, N 9.65, found: C 66.58, H 7.94, N 9.67.

4.1.2.9. 2-(1-Adamantyloxy)ethyl 5-aminoisoxazole-3-carboxylate ***(4l)***. Yellow solid (48 mg, 52%, A), mp: 178–179 °C, R_f (petroleum ether/EtOAc 2:1): 0.10; ^{1}H NMR (400.0 MHz, $CDCl_3$) (δ, ppm): 1.53–1.65 (m, 6H, $3CH_2$(Ad)), 1.70–1.75 (m, 6H, $3CH_2$(Ad)), 2.09–2.16 (m, 3H, 3CH (Ad)), 3.72 (t, J = 5.3 Hz, 2H, CH_2), 4.40 (t, J = 5.3 Hz, 2H, CH_2), 4.62 (br.s, 2H, NH_2), 5.52 (s, 1H, CH); ^{13}C NMR (100.6 MHz, $CDCl_3$) (δ, ppm): 30.5 (3CH(Ad)), 36.4 ($3CH_2$(Ad)), 41.4 ($3CH_2$(Ad)), 57.8 (CH_2O), 65.5 (CH_2O), 72.7 (C(Ad)), 80.7 (CH), 157.3 (C), 160.3 (C═O), 169.5 (C—NH_2); HRMS-ESI *m/z* $[M+Na]^+$ calcd for $C_{16}H_{22}N_2O_4Na^+$: 329.1472, found: 329.1471; Anal. calcd for $C_{16}H_{22}N_2O_4$: C 62.73, H 7.24, N 9.14, found: C 62.91, H 7.09, N 9.25.

4.1.2.10. 4-(1-Adamantyl)benzyl 5-aminoisoxazole-3-carboxylate ***(4m)***. Colourless solid (59 mg, 56%, A), mp: 168–170 °C, R_f (petroleum ether/EtOAc 4:1): 0.11; ^{1}H NMR (400.0 MHz, $CDCl_3$) (δ, ppm): 1.73–1.86 (m, 6H, CH_2(Ad)), 1.89–1.97 (m, 6H, CH_2(Ad)), 2.08–2.16 (m, 3H, 3CH (Ad)) 4.66 (br.s, 2H, NH_2), 5.36 (s, 2H, CH_2O), 5.55 (s, 1H, CH), 7.34–7.45 (m, 4H, 4CH(Ar)); ^{13}C NMR (100.6 MHz, $CDCl_3$) (δ, ppm): 28.9 (3CH(Ad)), 36.1 (C(Ad)), 36.7 ($3CH_2$(Ad)), 40.1 ($3CH_2$(Ad)), 67.4 (CH_2O), 80.7 (CH), 125.2 (2CH(Ar)), 128.6 (2CH(Ar)), 132.0 (C(Ar)), 151.9 (C(Ar)), 157.3 (C), 160.3 (C═O), 169.7 (C—NH_2); HRMS-ESI *m/z* $[M+Na]^+$ calcd for $C_{21}H_{24}N_2O_3Na^+$: 375.1679, found: 375.1672.

4.1.2.11. 1-Adamantylmethyl 5-amino-4-methylisoxazole-3-carboxylate ***(4n)***. Colourless solid (64 mg, 74%, B), mp: 189–190 °C, R_f (petroleum ether/EtOAc 4:1): 0.16; ^{1}H NMR (400.0 MHz, $CDCl_3$) (δ, ppm): 1.56–1.60 (m, 6H, $2CH_2$(Ad)), 1.60–1.67 (m, 3H, $3CH_2$(Ad)), 1.67–1.73 (m, 3H, $3CH_2$(Ad)), 1.93–1.98 (m, 3H, 3CH(Ad)), 1.99 (s, 3H, CH_3), 3.92 (s, 2H, CH_2), 3.73 (br. .s, 2H, NH_2); ^{13}C NMR (100.6 MHz, $CDCl_3$) (δ, ppm): 6.8 (CH_3), 27.9 (3CH(Ad)), 33.4 (C(Ad)), 36.8 ($3CH_2$(Ad)), 39.2 ($3CH_2$(Ad)), 74.9 (CH_2), 89.8 (C), 155.7 (C), 161.3 (C═O), 166.9 (CNH_2); HRMS-ESI *m/z* $[M+K]^+$ calcd for $C_{16}H_{22}N_2O_3K^+$: 329.1262, found: 329.1263; Anal. calcd for $C_{16}H_{22}N_2O_3$: C 66.18, H 7.64, N 9.65, found: C 66.19, H 7.68, N 9.59.

4.1.2.12. 1-Adamantylmethyl 5-amino-4-(2-phenylethyl)isoxazole-3-carboxylate ***(4o)***. Colourless solid (73 mg, 64%, B), mp: 155–157 °C, R_f (petroleum ether/EtOAc 4:1): 0.20; ^{1}H NMR (400.0 MHz, $CDCl_3$) (δ, ppm): 1.59–1.63 (m, 6H, $2CH_2$(Ad)), 1.63–1.68 (m, 3H, $3CH_2$(Ad)), 1.68–1.75 (m, 3H, $3CH_2$(Ad)), 1.96–2.02 (m, 3H, 3CH(Ad)), 2.71–2.78 (m, 2H, CH_2), 2.78–2.84 (m, 2H, CH_2), 3.67 (br. s, 2H, NH_2), 3.95 (s, 2H, CH_2), 7.09–7.14 (m, 2H, 2CH(Ar)), 7.16–7.23 (m, 1H, CH(Ar)), 7.24–7.29 (m, 2H, 2CH(Ar)); ^{13}C NMR (100.6 MHz, $CDCl_3$) (δ, ppm): 24.3 (CH_2), 27.9 (3CH(Ad)), 33.4 (C(Ad)), 36.1 (CH_2), 36.8 ($3CH_2$(Ad)), 39.2 ($3CH_2$(Ad)), 75.0 (CH_2), 93.9 (C), 126.3 (CH(Ar)), 128.6 (2CH(Ar)), 128.8 (2CH(Ar)), 141.5 (C(Ar)), 155.4 (C), 161.2 (C═

O), 167.7 (CNH_2); HRMS-ESI *m/z* $[M+K]^+$ calcd for $C_{23}H_{28}N_2O_3K^+$: 419.1732, found: 419.1727; Anal. calcd for $C_{23}H_{28}N_2O_3$: C 72.60, H 7.42, N 7.36, found: C 73.77, H 7.76, N 7.58.

4.2. Protocols of biological tests

4.2.1. Cells and viruses

Porcine embryo kidney (PEK) cell line was maintained at 37 °C in medium 199 (FSBSI "Chumakov FSC R&D IBP RAS", Russia) supplemented with 5% fetal bovine serum (FBS, Invitrogen, South America).

TBEV strain Absettarov (GenBank access no. KU885457) from laboratory collection was isolated in the Leningrad region, USSR, in 1951 from the blood of a patient with acute TBE. POWV strain Powassan 24 (GenBank access no. KU160627) from laboratory collection was isolated from *Ixodes persulcatus* ticks in Primorsky kray, USSR, in 1976. OHFV strain Nikitina (GenBank access no. GU290187) from laboratory collection was isolated in the Omsk region, USSR, in 1948 from the blood of a patient with Omsk hemorrhagic fever.

Viruses were stored as aliquots of infected cultural fluid at −70 °C.

4.2.2. Cytotoxicity test in PEK cells

The test was performed as described previously [4] with some changes. Two-fold dilutions of studied compounds were prepared in medium 199 on Earle solution (FSBSI "Chumakov FSC R&D IBP RAS", Russia) in 96-well plates to obtain final concentrations starting from 500 μM. Equal 100 μL aliquots of compound dilutions were added in three replicates to each well of 96-well plates with PEK cell monolayers. Negative control cells were treated with the same sequential concentrations of DMSO, as it was in compound dilutions, or cultural medium with no additions. After incubation at 37 °C in CO_2-incubator on days 1 or 7 cultural supernatant was gently removed and the cells were washed with phosphate buffered saline (PBS, Sigma) twice. Solution of 0.0002% neutral red in PBS was added to the washed cells, and cells were incubated for 30 min at 37 °C in CO_2-incubator. Afterwards cells were gently washed with PBS twice and 100 μL of 96% ethanol were added. Absorption was counted in MultiScan FC (Thermo) at 450 nm. CC_{50} was calculated according to Reed-and-Muench method [36].

4.2.3. 50% plaque reduction test

The test was performed as described previously [4] with some changes. Four 4-fold dilutions of studied compounds were prepared in medium 199 on Earle solution (FSBSI "Chumakov FSC R&D IBP RAS", Russia) to obtain final concentrations in the wells starting from 50 μM. Equal volume of TBEV or POWV suspension, containing approximately 20–30 PFU, were added to each compound dilution. Control virus was added to the same sequential dilutions of DMSO, as it was in compounds dilutions. Virus + compound and virus + DMSO mixtures were incubated at 37 °C in CO_2-incubator for 1 h and then added to 24-well plates with PEK cell monolayers in 2 replicates, and incubated at 37 °C in CO_2-incubator for 1 h with gentle shaking. Then, each well was overlaid with 0.85–1.26% methylcellulose (Sigma) containing 2% FBS (Invitrogen, South America). After incubation at 37 °C in CO_2-incubator for 6 days cells were fixed with 96% ethanol, and foci were stained with 0.4% gentian violet and counted. EC_{50} values for TBEV were calculated according to Reed-and-Muench method [36] and for OHFV and POWV were estimated from the linear fitting of the inhibition curves with OriginLab Corporation OriginPro 8.

N-Butyl-2-methyl-5,6,7,8-tetrahydroquinazoline-4-amine 1-oxide, described previously [12], was used as the reference compound.

4.2.4. 'Time of addition' experiments.

PEK cells were infected with TBEV strain Absettarov (MOI 0.1 PFU/cell) and treated with 5 × EC_{50} compound or DMSO (negative control) solution addition according to one of the schemes:

(1) Cells were incubated with 5 × EC_{50} compound / DMSO solution for 2 h, washed and then infected with virus;
(2) Virus was incubated with 5 × EC_{50} compound / DMSO solution for 2 h prior to infection of the cells;
(3) 5 μM compound / DMSO solution was added to the cells 2 h.p.i.;
(4) 5 μM compound / DMSO solution was added to the cells 5 h.p.i.

In all the schemes virus was left with the cells for 2 h for sorption and entry, and then cell monolayers were washed from unsorbed virus. Each experimental scheme was performed in two replicates. Infected cell culture supernates were harvested 21 h.p.i., and viral yields were determined by plaque formation assay under 1.26% methylcellylose (Sigma), supplemented with 2% FBS (Invitrogen, South America). On the 6th day post infection plaques were stained with 0.6% gentian violet and counted; virus yields were expressed as lgPFU. Inhibition of viral reproduction was estimated as the difference between DMSO-treated control and compound-treated cells for each scheme.

4.3. Molecular docking

Molecular docking was performed according to the protocol described in ref. [12]. Conformational generation for small molecules was performed in OMEGA 2.4.6 [37,38], partial atomic charges were calculated in QUACPAC 1.5.0 [39], docking was performed with FRED 2.2.5 [40,41]. Fig. 3 was rendered in VIDA 4.3.0 [42].

4.4. Prediction of ADMET profiles and physico-chemical properties

The human intestinal absorption (HIA) [18], blood-brain barrier permeability (LogBB) [19], and hERG-mediated cardiac toxicity risk (channel affinity pK_i and inhibitory activity pIC_{50}) [20] were estimated using the integrated online service for ADMET properties prediction [43]. It implements the predictive QSAR models based on the accurate and representative training sets, fragmental descriptors, and artificial neural networks. The lipophilicity ($logP_{ow}$) for the neutral compound and the aqueous solubility (pS) were estimated by the ALogPS 3.0 neural network model based on the E-State descriptors implemented in the OCHEM platform [21].

Acknowledgements

The antiviral activity studies were supported by the Russian Science Foundation (grant no. 16-15-10307). Compound synthesis was supported by IPhAC RAS program 45.5 and the Russian Foundation for Basic Research (projects 18-03-00651 and 18-03-00524). Free academic license for QUACPAC, OMEGA, FRED, and VIDA was kindly provided by OpenEye Scientific Software Inc. The authors appreciate technical assistance by Alexey A. Orlov and calculation of ADMET parameters by Dr. Eugene V. Radchenko.

Appendix A. Supplementary material

Supplementary data to this article can be found online at https://doi.org/10.1016/j.bioorg.2019.03.028.

References

[1] D. Ruzek, T. Avšič Županc, J. Borde, A. Chrdle, L. Eyer, G. Karganova, I. Kholodilov, N. Knap, L. Kozlovskaya, A. Matveev, A.D. Miller, D.I. Osolodkin, A.K. Överby, N. Tikunova, S. Tkachev, J. Zajkowska, Tick-borne encephalitis in Europe and Russia: review of pathogenesis, clinical features, therapy, and vaccines, Antivir. Res. 164 (2019) 23–51, https://doi.org/10.1016/j.antiviral.2019.01.014.
[2] G. Kemenesi, K. Bányai, Tick-borne flaviviruses, with a focus on powassan virus, Clin. Microbiol. Rev. 32 (2019) e00106-17.
[3] S. Mukhopadhyay, R.J. Kuhn, M.G. Rossmann, A structural perspective of the *Flavivirus* life cycle, Nat. Rev. Microbiol. 3 (2005) 13–22.
[4] D.I. Osolodkin, L.I. Kozlovskaya, E.V. Dueva, V.V. Dotsenko, Y.V. Rogova, K.A. Frolov, S.G. Krivokolysko, E.G. Romanova, A.S. Morozov, G.G. Karganova,

V.A. Palyulin, V.M. Pentkovski, N.S. Zefirov, Inhibitors of tick-borne flavivirus reproduction from structure-based virtual screening, ACS Med. Chem. Lett. 4 (9) (2013) 869–874.
[5] Fields Virology vol. 1, (2013) 747–794.
[6] G.V. Proskurin, A.A. Orlov, V.A. Brylev, L.I. Kozlovskaya, A.A. Chistov, G.G. Karganova, V.A. Palyulin, D.I. Osolodkin, V.A. Korshun, A.V. Aralov, 3′-O-Substituted 5-(perylen-3-ylethynyl)-2′-deoxyuridines as tick-borne encephalitis virus reproduction inhibitors, Eur. J. Med. Chem. 155 (2018) 77–83.
[7] A.A. Orlov, A.A. Eletskaya, K.A. Frolov, A.D. Golinets, V.A. Palyulin, S.G. Krivokolysko, L.I. Kozlovskaya, V.V. Dotsenko, D.I. Osolodkin, Probing chemical space of tick-borne encephalitis virus reproduction inhibitors with organoselenium compounds, Arch. Pharm. Chem. Life Sci. 351 (6) (2018) e1700353.
[8] L.I. Kozlovskaya, A.D. Golinets, A.A. Eletskaya, A.A. Orlov, V.A. Palyulin, S.N. Kochetkov, L.A. Alexandrova, D.I. Osolodkin, Selective inhibition of *enterovirus a* species members' reproduction by furano[2, 3-*d*]pyrimidine nucleosides revealed by antiviral activity profiling against (+)ssRNA viruses, Chem. Select. 3 (2018) 2321–2325.
[9] A.A. Orlov, M.S. Drenichev, V.E. Oslovsky, N.N. Kurochkin, P.N. Solyev, L.I. Kozlovskaya, V.A. Palyulin, G.G. Karganova, S.N. Mikhailov, D.I. Osolodkin, New tools in nucleoside toolbox of tick-borne encephalitis virus reproduction inhibitors, Bioorg. Med. Chem. Lett. 27 (2017) 1267–1273.
[10] A.V. Aralov, G.V. Proskurin, A.A. Orlov, L.I. Kozlovskaya, A.A. Chistov, S.V. Kutyakov, G.G. Karganova, V.A. Palyulin, D.I. Osolodkin, V.A. Korshun, Perylenyltriazoles inhibit reproduction of enveloped viruses, Eur. J. Med. Chem. 138 (2017) 293–299.
[11] A.A. Orlov, A.A. Chistov, L.I. Kozlovskaya, A.V. Ustinov, V.A. Korshun, G.G. Karganova, D.I. Osolodkin, Rigid amphipathic nucleosides suppress reproduction of the tick-borne encephalitis virus, Med. Chem. Commun. 7 (2016) 495–499.
[12] K.N. Sedenkova, E.V. Dueva, E.B. Averina, Y.K. Grishin, D.I. Osolodkin, L.I. Kozlovskaya, V.A. Palyulin, E.N. Savelyev, B.S. Orlinson, I.A. Novakov, G.M. Butov, T.S. Kuznetsova, G.G. Karganova, N.S. Zefirov, Synthesis and assessment of 4-aminotetrahydroquinazoline derivatives as tick-borne encephalitis virus reproduction inhibitors, Org. Biomol. Chem. 13 (2015) 3406–3415.
[13] Y.A. Volkova, E.B. Averina, D.A. Vasilenko, K.N. Sedenkova, Y.K. Grishin, P. Bruheim, T.S. Kuznetsova, N.S. Zefirov, Unexpected heterocyclization of electrophilic alkenes by tetranitromethane in the presence of triethylamine. Synthesis of 5-nitroisoxazoles, J. Org. Chem. 84 (2019) 3192–3200.
[14] E.B. Averina, Y.A. Volkova, Y.V. Samoilichenko, Y.K. Grishin, V.B. Rybakov, A.G. Kutateladze, M.E. Elyashberg, T.S. Kuznetsova, N.S. Zefirov, Heterocyclization of electrophilic alkenes with tetranitromethane revisited: regiochemistry and the mechanism of nitroisoxazole formation, Tetrahedron Lett. 53 (2012) 1472–1475.
[15] E.B. Averina, D.A. Vasilenko, Y.V. Samoilichenko, Y.K. Grishin, V.B. Rybakov, T.S. Kuznetsova, N.S. Zefirov, Chemoselective reduction of functionalized 5-nitroisoxazoles: synthesis of 5-amino- and 5-[hydroxy(tetrahydrofuran-2-yl)amino] isoxazoles, Synthesis 46 (2014) 1107–1113.
[16] E.B. Averina, D.A. Vasilenko, Y.A. Gracheva, Y.K. Grishin, E.V. Radchenko, V.V. Burmistrov, G.M. Butov, M.E. Neganova, T.P. Serkova, O.M. Redkozubova, E.F. Shevtsova, E.R. Milaeva, T.S. Kuznetsova, N.S. Zefirov, Synthesis and biological evaluation of novel 5-hydroxylaminoisoxazole derivatives as lipoxygenase inhibitors and metabolism enhancing agents, Bioorg. Med. Chem. 24 (2016) 712–720.
[17] D.A. Vasilenko, E.B. Averina, N.A. Zefirov, B. Wobith, Y.K. Grishin, V.B. Rybakov, O.N. Zefirova, T.S. Kuznetsova, S.A. Kuznetsov, N.S. Zefirov, Synthesis and antimitotic activity of novel 5-aminoisoxazoles bearing alkoxyaryl moieties, Mendeleev Commun. 27 (2017) 228–230.
[18] E.V. Radchenko, A.S. Dyabina, V.A. Palyulin, N.S. Zefirov, Prediction of human intestinal absorption of drug compounds, Russ. Chem. Bull. 65 (2016) 576–580, https://doi.org/10.1007/s11172-016-1340-0.
[19] A.S. Dyabina, E.V. Radchenko, V.A. Palyulin, N.S. Zefirov, Prediction of blood-brain barrier permeability of organic compounds, Dokl. Biochem. Biophys. 470 (2016) 371–374, https://doi.org/10.1134/S1607672916050173.
[20] E.V. Radchenko, Y.A. Rulev, A.Y. Safanyaev, V.A. Palyulin, N.S. Zefirov, Computer-aided estimation of the hERG-mediated cardiotoxicity risk of potential drug components, Dokl. Biochem. Biophys. 473 (2017) 128–131, https://doi.org/10.1134/S1607672917020107.
[21] I. Sushko, S. Novotarskyi, R. Koerner, A.K. Pandey, M. Rupp, W. Teetz, S. Brandmaier, A. Abdelaziz, V.V. Prokopenko, V.Y. Tanchuk, R. Todeschini, A. Varnek, G. Marcou, P. Ertl, V. Potemkin, M. Grishina, J. Gasteiger, C. Schwab, I.I. Baskin, V.A. Palyulin, E.V. Radchenko, W.J. Welsh, V. Kholodovych, D. Chekmarev, A. Cherkasov, J. Aires-de-Sousa, Q.Y. Zhang, A. Bender, F. Nigsch, L. Patiny, A. Williams, Tkachenko V., Tetko I.V., Online chemical modeling environment (OCHEM): web platform for data storage, model development and publishing of chemical information, J. Comp. – Aided Mol. Des. 25 (6) (2011) 533–554, https://doi.org/10.1007/s10822-011-9440-2.
[22] W. Wang, Y. Li, M. Sun, C. Zhou, Y. Zhang, Y. Lia, Q. Yang, Colorimetric and fluorescent nanofibrous film as a chemosensor for Hg^{2+} in aqueous solution prepared by electrospinning and host–guest interaction, Chem. Commun. 48 (2012) 6040–6042.
[23] V.F. Baklan, A.N. Khil'chevskii, V.M. D'yakovskaya, L.S. Sologub, V.P. Kukhar, Reaction of alcohols with bromine, Russ. J. Org. Chem. 29 (3) (1993) 454–456.
[24] J. Schraml, J. Vcelak, V. Chvalovsky, G. Engelhardt, H. Jancke, L. Vodicka, J. Hlavaty, ^{29}Si and ^{13}C-NMR spectra and steric effects in mono- and bis(trimethylsiloxy)adamantanes, Collect. Czech. Chem. Commun. 43 (1978) 3179.
[25] G. Anderson, W. Burks, I. Harruna, Novel synthesis of 3-fluoro-1-aminoadamantane and some of its derivatives, Synth. Commun. 18 (1988) 1967–1974.
[26] P. Kadaba, A convenient method of esterification of unsaturated organic acids using a boron trifluoride etherate-alcohol, Reagent. Synthesis 6 (1971) 316–317.
[27] M.V. Avdeev, E.I. Bagrii, G.B. Maravin, Y.M. Korolev, R.S. Borisov, Oxidation of cycloalkanes with potassium peroxosulfate catalyzed by montmorillonite-immobilized metal tetrapyridylporphyrin complexes, Petrol. Chem. 40 (2000) 391–398.
[28] Y.N. Klimochkin, E.I. Bagrii, T.N. Dolgopolova, I.K. Moiseev, Synthesis of alkoxycarbonylaminoadamantanes and acetylamino-adamantanes in nitric acid, Bull. Acad. Sci. USSR, Div. Chem. Sci. (Engl. Transl.) 37 (4) (1988) 757–759.
[29] L. Wanka, C. Cabrele, M. Vanejews, P.R. Schreiner, γ-aminoadamantanecarboxylic acids through direct C–H bond amidations, Eur. J. Org. Chem. 2007 (9) (2007) 1474–1490.
[30] S.A. Lipton, G.T. Went (Wilson Sonsini Goodrich & Rosati Adamas Pharmaceuticals, Ink., USA) US Patent No US20100137448 A1, 2010.
[31] O.N. Zefirova, E.V. Nurieva, H. Lemcke, A.A. Ivanov, N.V. Zyk, D.G. Weiss, S.A. Kuznetsov, N.S. Zefirov, Design, synthesis and bioactivity of simplified taxol analogues on the basis of bicyclo[3.3.1]nonane derivatives, Mendeleev Commun. 18 (2008) 183–186.
[32] D.J. Augeri, J.A. Robl, D.A. Betebenner, D.R. Magnin, A. Khanna, J.G. Robertson, A. Wang, L.M. Simpkins, P. Taunk, Q. Huang, S.-P. Han, B. Abboa-Offei, M. Cap, L. Xin, L. Tao, E. Tozzo, G.E. Welzel, D.M. Egan, J. Marcinkeviciene, S.Y. Chang, S.A. Biller, M.S. Kirby, R.A. Parker, L.G. Hamann, Discovery and preclinical profile of saxagliptin (BMS-477118): a highly potent, long-acting, orally active dipeptidyl peptidase IV inhibitor for the treatment of type 2 diabetes, J. Med. Chem. 48 (2005) 5025–5037.
[33] N. Takahashi, D. Mochizuki, (Asahi chemical ind., Japane) US Patent No. US5658923 (A), 1997.
[34] A.N. Reznikov, M.Y. Skomorokhov, Y.N. Klimochkin, Synthesis of 1-adamantyloxyalkanols, Russ. J. Org. Chem. 46 (2010) 1741–1742.
[35] F.N. Stepanov, E.J. Dikolereko, G.J. Danilenko, Adamantane and its derivatives VI. Substitution reactions in aryladamantanes. Zh. Org. Khim. 2 (4) (1966) 640–643, Chem. Abstr. 65 (6) (1966) 8782h.
[36] L.J. Reed, H. Muench, A simple method of estimating fifty per cent endpoints, Am. J. Epidemiol. 27 (1938) 493.
[37] OMEGA, version 2.4.6, OpenEye Scientific Software, Inc., Santa Fe, NM, USA, 2010. http://www.eyesopen.com.
[38] P.C.D. Hawkins, A.G. Skillman, G.L. Warren, B.A. Ellingson, M.T. Stahl, Conformer generation with OMEGA: algorithm and validation using high quality structures from the protein databank and Cambridge structural database, J. Chem. Inf. Model. 50 (2010) 572.
[39] QUACPAC, version 1.5.0, OpenEye Scientific Software, Inc., Santa Fe, NM, USA, 2010. http://www.eyesopen.com.
[40] FRED, version 2.2.5, OpenEye Scientific Software, Inc., Santa Fe, NM, USA, 2010. http://www.eyesopen.com.
[41] M. McGann, FRED and HYBRID docking performance on standardized datasets, J. Comput. Aided Mol. Des. 26 (2012) 897–909.
[42] VIDA, version 4.3.0, OpenEye Scientific Software, Inc., Santa Fe, NM, USA, 2014. http://www.eyesopen.com.
[43] ADMET Prediction Service. http://qsar.chem.msu.ru/admet/ (accessed 01 Feb 2019).